EMRP Project - Metrology for Drug Delivery

WP2, deliverable 2.1.3 – Report v1

Numerical simulations of pulsating flow in nano-flow facility of DTI

Jan Geršl

Czech metrology institute

The research leading to the results discussed in this report has received funding from the European Metrology Research Programme (EMRP). The EMRP is jointly funded by the EMRP participating countries within Euramet and the European Union.

1 Introduction

In this work we develop a physical model which describes behaviour of the gravimetric nano-flow facility of DTI. The aim of this model is to predict effects which occur in the system in case when the flow coming into the system is oscillating.
The model covers evolution of the main disturbing forces which occur during weighing, namely capillary forces between the tube inserted into the beaker and interfaces of fluids in the beaker (air-oil, oil-water) and buoyancy force between the tube and the fluids. Influence of these forces to the scale reading is predicted too.
The physical model is implemented into Matlab and a difference between the real oscillating flowrate and its apparent value obtained by time derivative of scale reading is computed numerically.
Time needed for stabilization of the system is discussed too.

2 Physical model

In [1] we found that the leading error sources during a weighing of liquid in a beaker with a tube inserted inside the fluid are the capillary forces acting at contact lines of liquid to liquid interfaces with the tube and a buoyancy force acting to the tube. Determination of these forces requires knowledge of evolution of shape of the interfaces during the pulsating flow.
In the following work we assume that even for pulsating flow the surface shape is given by equation for an equilibrium case with no flow where the dynamics enters only through a dynamic behaviour of the contact angles which depend on a velocity of the contact line between the interface and the tube.
This assumption is correct if 1) the fluid velocity field in surroundings of the interface does not affect the interface shape significantly and 2) reaction of the surface shape to a change of contact angle is almost immediate, or more precisely a stabilisation time of the surface shape after a step change in contact angles from values corresponding to a constant flowrate Q to values corresponding to $Q+A_Q$, where A_Q is a flowrate amplitude of the considered pulsating flow, is much smaller than a period of the pulsating flow.
In this case the surface shape is given as a solution of equation (3.8) from [1]

$$C + Bf(r) = \frac{1}{r}\frac{d}{dr}\left(r\frac{df/dr}{\sqrt{1+(df/dr)^2}}\right), \tag{2.1}$$

where $B = (\rho_{F2} - \rho_{F1})g/\gamma$ is a constant with ρ_{F1} being a density of fluid above the interface, ρ_{F2} being a density of fluid below the interface, g being a gravitational acceleration and γ being a surface tension of the interface. The function $f(r)$ describes a shape of the interface. This function gives height of the interface point at radius r above certain level. In [1] the level was selected as the contact point of the interface with the tube such that at the tube we have $f(r) = 0$. Here it will be more convenient to choose the level as a fixed point without reference to the interface – e.g. as a bottom of the beaker (see Fig. 1). If we do so the constant C is given as

$$C = (p_{F1}^0 - p_{F2}^0)/\gamma - Bf(a) \tag{2.2}$$

where a is the outer radius of the tube, p_{F1}^0 is a pressure of the fluid immediately above the contact line at the tube and p_{F2}^0 is a pressure of the fluid immediately below the contact line at the tube.

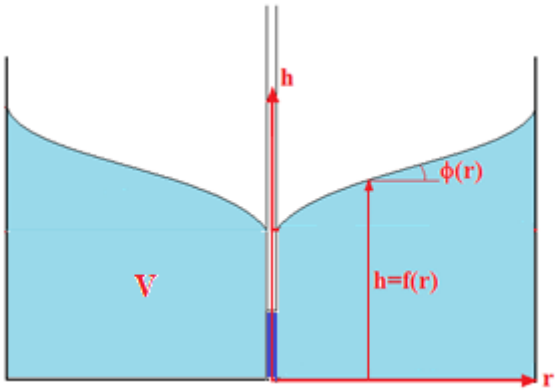

Fig. 1

If we consider densities of water $\rho_W = 997\ kg/m^3$, of oil $\rho_O = 890\ kg/m^3$ and of air $\rho_A = 1.2\ kg/m^3$, surface tensions $\gamma_{AO} = 0.026\ N/m$, $\gamma_{OW} = 0.041\ N/m$ and $g = 9.81\ ms^{-2}$ for oil-water interface we obtain $B_{OW} = 0.0256\ mm^{-2}$ and for air-oil interface we get $B_{AO} = 0.335\ mm^{-2}$.
For a volume under the interface (the light blue in Fig. 1) we have

$$V = 2\pi \int_a^R f(r) r dr \tag{2.3}$$

and again as in [1] by integrating the equation (2.1) we obtain

$$C\pi(R^2 - a^2) + BV = 2\pi(R \sin\phi(R) - a \sin\phi(a)) \tag{2.4}$$

where the angles $\phi(r)$ are defined in Fig. 1 and R is the inner radius of the beaker. The dimensions of the setup are a = 0.4 mm and R = 10 mm. The angles ϕ are related to contact angles as $\theta(a) = \phi(a) + \pi/2$ and $\theta(R) = \pi/2 - \phi(R)$. The term $\pi(R^2 - a^2)$ is just surface of the cross-section of the beaker without the cross-section of the tube and we denote it

$$S = \pi(R^2 - a^2). \tag{2.5}$$

Therefore the parameter C can be expressed from (2.4) as

$$C = \frac{1}{S}\left(-BV + 2\pi(R\cos\theta(R) + a\cos\theta(a))\right). \tag{2.6}$$

The strategy to obtain the evolution of capillary and buoyancy forces in case of pulsating flow will be following. If we know the volume under the interface V and the contact angles $\theta(a)$ and $\theta(R)$ we can use the equation (2.6) to calculate the parameter C and then solve the equation (2.1) for boundary conditions

$$\frac{df}{dr}(a) = \tan\phi(a) = \tan\left(\theta(a) - \frac{\pi}{2}\right) \tag{2.7}$$

$$\frac{df}{dr}(R) = \tan\phi(R) = \tan(\pi/2 - \theta(R)).$$

In the following we will denote $\theta(a) = \theta_1$ and $\theta(R) = \theta_2$. The solution of equation (2.1) for given volume and contact angles we denote $f(r, \cos\theta_1, \cos\theta_2, V)$ where we write cosines of contact angles instead of contact angles themselves since it will be convenient as we will see.
Next we consider a time dependent volume $V = V_0 + V(t)$ where V_0 is initial value of volume under the interface and $V(t)$ is a time dependent change of volume in the beaker. Since the interface for given contact angles and different volumes is just shifted in height without change in shape we have

$$f\big(r,\cos\theta_1,\cos\theta_2,V_0+V(t)\big)=f(r,\cos\theta_1,\cos\theta_2,V_0)+\frac{V(t)}{S}. \tag{2.8}$$

Now we introduce the dependence of contact angles on the velocity of the contact line between the interface and the tube. Some theoretical and experimental models of this dependence can be found e.g. in [2]. All the relations mentioned in this reference are of form $\cos\theta=\cos\theta_0+\Delta(\dot{h})$ where $\theta_0$is the equilibrium contact angle for the static case and $\Delta(\dot{h})$ is some function of the contact line velocity which is given as a time derivative of height of the contact line in our case. In our situation we have two contact lines at one interface and we can write

$$\begin{aligned}\cos\theta_1&=\cos\theta_{01}+\Delta_1\big(\dot{h}_1\big)\\ \cos\theta_2&=\cos\theta_{02}+\Delta_2\big(\dot{h}_2\big)\end{aligned} \tag{2.9}$$

where the indices 1 relates to the tube wall whereas the indices 2 relates to the beaker wall.
The height of the contact lines as a function of time is in our case given as

$$\begin{aligned}h_1(t)&=f\big(a,\cos\theta_1,\cos\theta_2,V_0+V(t)\big)\\ &=f\big(a,\cos\theta_{01}+\Delta_1\big(\dot{h}_1(t)\big),\cos\theta_{02}+\Delta_2\big(\dot{h}_2(t)\big),V_0\big)+\frac{V(t)}{S}\\ h_2(t)&=f\big(R,\cos\theta_1,\cos\theta_2,V_0+V(t)\big)\\ &=f\big(R,\cos\theta_{01}+\Delta_1\big(\dot{h}_1(t)\big),\cos\theta_{02}+\Delta_2\big(\dot{h}_2(t)\big),V_0\big)+\frac{V(t)}{S}.\end{aligned} \tag{2.10}$$

If the functions $f(a,\cos\theta_1,\cos\theta_2,V_0)$ and $f(R,\cos\theta_1,\cos\theta_2,V_0)$ are known these two equations can be considered as a set of differential equations for unknown functions $h_1(t)$, $h_2(t)$. Solving these equations we obtain all the information needed for determining the capillary and buoyancy forces as we will see later.
The functions $f(a,\cos\theta_1,\cos\theta_2,V_0)$ and $f(R,\cos\theta_1,\cos\theta_2,V_0)$ have to be obtained numerically by solving the equation (2.1) and therefore it is difficult to handle with them in further computations. However, we can suppose that the corrections $\Delta_1\big(\dot{h}_1\big)$ and $\Delta_2\big(\dot{h}_2\big)$ are small enough to make a linear expansion of the functions $f(a,\cos\theta_1,\cos\theta_2,V_0)$ and $f(R,\cos\theta_1,\cos\theta_2,V_0)$ in variables $\cos\theta_1$ and $\cos\theta_2$. Let us denote

$$\begin{aligned}h_{01}&=f(a,\cos\theta_{01},\cos\theta_{02},V_0)\\ h_{02}&=f(R,\cos\theta_{01},\cos\theta_{02},V_0)\\ c_{11}&=\frac{\partial f(a,\cos\theta_1,\cos\theta_{02},V_0)}{\partial\cos\theta_1}\Big|_{\theta_1=\theta_{01}}\\ c_{12}&=\frac{\partial f(a,\cos\theta_{01},\cos\theta_2,V_0)}{\partial\cos\theta_2}\Big|_{\theta_2=\theta_{02}}\\ c_{21}&=\frac{\partial f(R,\cos\theta_1,\cos\theta_{02},V_0)}{\partial\cos\theta_1}\Big|_{\theta_1=\theta_{01}}\\ c_{22}&=\frac{\partial f(R,\cos\theta_{01},\cos\theta_2,V_0)}{\partial\cos\theta_2}\Big|_{\theta_2=\theta_{02}}.\end{aligned} \tag{2.11}$$

With this notation we can write the linear expansion of the equations (2.10) as

$$h_1(t)=h_{01}+c_{11}\Delta_1\big(\dot{h}_1(t)\big)+c_{12}\Delta_2\big(\dot{h}_2(t)\big)+V(t)/S \tag{2.12}$$

$$h_2(t) = h_{02} + c_{21}\Delta_1\big(\dot{h}_1(t)\big) + c_{22}\Delta_2\big(\dot{h}_2(t)\big) + V(t)/S.$$

We can introduce quantities

$$\bar{h}_1(t) = h_1(t) - h_{01} \tag{2.13}$$
$$\bar{h}_2(t) = h_2(t) - h_{02} \tag{2.14}$$

and rewrite the equations (2.12) as explicit expressions for the derivative terms

$$\Delta_1\left(\dot{\bar{h}}_1(t)\right) = \frac{1}{c_{11}c_{22} - c_{12}c_{21}}\left(c_{22}\bar{h}_1(t) - c_{12}\bar{h}_2(t) - (c_{22} - c_{12})\,V(t)/S\right) \tag{2.15}$$

$$\Delta_2\left(\dot{\bar{h}}_2(t)\right) = \frac{-1}{c_{11}c_{22} - c_{12}c_{21}}\left(c_{21}\bar{h}_1(t) - c_{11}\bar{h}_2(t) - (c_{21} - c_{11})\,V(t)/S\right).$$

The equations (2.15) should be solved for $\bar{h}_1(t)$ and $\bar{h}_2(t)$ with initial conditions $\bar{h}_1(0) = \bar{h}_2(0) = 0$. The function $V(t)$ in (2.15) describes the pulsating flow and is given as an input. The coefficients c_{11}, c_{12}, c_{21}, c_{22} must be determined numerically by solving the equation (2.1) for various contact angles. If we want to obtain the variables $h_1(t)$, $h_2(t)$ we need to find also the coefficients h_{01}, h_{02} by solving the equation (2.1) numerically. For determining these coefficients we need to know the equilibrium contact angles $\theta_{01}$and θ_{02} which have to be determined by experiment or from literature.
Regarding the functions Δ_1 and Δ_2 there are several models how they should look like. The models are summarised in [2]. From the models mentioned in this reference the best theoretical model is the Blake model which gives

$$\Delta(\dot{h}) = -\frac{1}{D}\operatorname{arcsinh}(\dot{h}/A) \tag{2.16}$$

where *A*, *D* are constants given by some molecular characteristics of the fluids which are difficult to determine and therefore it is usually necessary to find them by fitting the model to some experimental data.
The best experimental model mentioned in [2] is the Seeberg model. The formula for Seeberg model in [2] is however valid probably only for air-liquid interfaces and gives

$$\Delta(\dot{h}) = -(\cos\theta_0 + 1)\,4.47\left(\frac{\mu\dot{h}}{\gamma}\right)^{0.42} \tag{2.17}$$

where γ is the surface tension and μ is a dynamical viscosity or the liquid. This formula is based on experimental data in a range

$$10^{-7} < \frac{\mu\dot{h}}{\gamma} < 10^{-3}. \tag{2.18}$$

The functions for Blake and Seeberg model are different. They can be fitted in certain range of $\dot{h}$ but especially for small values of $\dot{h}$ the difference can be significant because the derivative $d\Delta(\dot{h})/d\dot{h}$ for $\dot{h}$ approaching zero gives finite value for Blake model but for Seeberg model it approaches infinity.
Therefore it is important to have some experimental data from our own setup.

Now we will show how to calculate the capillary and buoyancy forces. We choose a *z*-axis oriented in the same way as the *h*-axis in Fig. 1 and we evaluate the *z*-component of the capillary and buoyancy forces acting to our system (as defined by Fig. 1 of [1]).
Let us suppose that we solved the equations (2.15) for both interfaces air-oil (AO) and oil-water (OW). Thus, we know the functions $\bar{h}_{1AO}(t)$, $\bar{h}_{2AO}(t)$, $\bar{h}_{1OW}(t)$ and $\bar{h}_{2OW}(t)$ and we know their time derivatives. From relations (2.9) we can calculate the cosines of contact angles.
The *z*-components of the capillary forces by which the tube acts to the liquids then are

$$F_{cAO}(t) = 2\pi a\gamma_{AO}\cos\theta_{1AO} = 2\pi a\gamma_{AO}\left(\cos\theta_{01AO} + \Delta_{1AO}(\dot{\bar{h}}_{1AO}(t))\right) \tag{2.19}$$
$$F_{cOW}(t) = 2\pi a\gamma_{OW}\cos\theta_{1OW} = 2\pi a\gamma_{OW}\left(\cos\theta_{01OW} + \Delta_{1OW}(\dot{\bar{h}}_{1OW}(t))\right).$$

The *z*-component of the buoyancy force acting to the system is expressed by formula (4.5) of [1]. The formula reads

$$F_b = -(\Delta p_{AO} + h_O\rho_O g + \Delta p_{OW} + h_W\rho_W g)\pi a^2 + V'\rho_A g \tag{2.20}$$

where $\Delta p_{AO} = p_O^0 - p_A^0$ is a pressure step when we pass through the air-oil interface at the wall of the tube, $\Delta p_{OW} = p_W^0 - p_O^0$ is a pressure step when we pass through the oil-water interface at the wall of the tube, h_O, h_W are defined in Fig. 2, ρ_O, ρ_W, ρ_A are densities of oil, water and air and V' is volume of the beaker plus the liquid inside the beaker plus the part of the tube which is inserted into the liquid. Now we have to express the formula (2.20) in terms of the functions $\bar{h}_{1AO}(t)$, $\bar{h}_{2AO}(t)$, $\bar{h}_{1OW}(t)$, $\bar{h}_{2OW}(t)$ and their time derivatives. The way of expressing Δp_{AO} and Δp_{OW} is the following. First we use the formulas (2.9) to express the $\cos\theta_1(t)$ and $\cos\theta_2(t)$. Then we use the formula (2.6) to express the parameter *C* which is related to the pressure step by formula (2.2). After some algebra we obtain the following formula for a pressure step

$$\Delta p = \frac{\gamma}{S}\Big(B\left(V_0 + V(t) - Sh_1(t)\right) - 2\pi(R\cos\theta_2(t) + a\cos\theta_1(t))\Big) \tag{2.21}$$

which for particular interfaces in terms of functions $\bar{h}_{1AO}(t)$, $\bar{h}_{2AO}(t)$, $\bar{h}_{1OW}(t)$, $\bar{h}_{2OW}(t)$ reads

$$\begin{aligned}
\Delta p_{OW} = \frac{\gamma_{OW}}{S}\Bigg(&B_{OW}\left(V_{0OW} + V(t) - S\left(h_{01OW} + \bar{h}_{1OW}(t)\right)\right)\\
&- 2\pi\left(R\left(\cos\theta_{02OW} + \Delta_{2OW}(\dot{\bar{h}}_{2OW}(t))\right) + a\left(\cos\theta_{01OW} + \Delta_{1OW}(\dot{\bar{h}}_{1OW}(t))\right)\right)\Bigg)\\
\Delta p_{AO} = \frac{\gamma_{AO}}{S}\Bigg(&B_{AO}\left(V_{0AO} + V(t) - S\left(h_{01AO} + \bar{h}_{1AO}(t)\right)\right)\\
&- 2\pi\left(R\left(\cos\theta_{02AO} + \Delta_{2AO}(\dot{\bar{h}}_{2AO}(t))\right) + a\left(\cos\theta_{01AO} + \Delta_{1AO}(\dot{\bar{h}}_{1AO}(t))\right)\right)\Bigg).
\end{aligned} \tag{2.22}$$

The heights h_O and h_W in formula (2.20) can be expressed as

$$\begin{aligned}
h_W &= h_{1OW} - h_{tip} = h_{01OW} + \bar{h}_{1OW}(t) - h_{tip}\\
h_O &= h_{1AO} - h_{1OW} = h_{01AO} + \bar{h}_{1AO}(t) - h_{01OW} - \bar{h}_{1OW}(t)
\end{aligned} \tag{2.23}$$

where h_{tip} is distance of the tip of the tube from bottom of the beaker.
Finally the volume V' reads

$$V' = V_B + V_{0AO} + V(t) + \pi a^2\left(h_{01AO} + \bar{h}_{1AO}(t)\right) \tag{2.24}$$

where V_B is volume of the beaker itself – i.e. the volume of glass of the beaker.

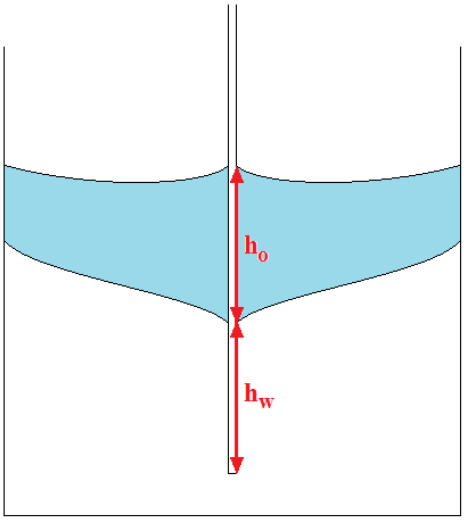

Fig. 2

The z-component of the gravitational force acting to the system is

$$F_g = -mg = -g\left(m_B + \rho_O V_O + \rho_W\left(V_{0OW} + V(t) + \pi a^2 h_{tip}\right)\right) \tag{2.25}$$

where m is a mass of the system, m_B is a mass of the beaker itself and V_O is the volume of oil which is constant. The real mass flowrate to the system is given as

$$Q = \frac{dm}{dt} = -\frac{1}{g}\frac{dF_g}{dt}. \tag{2.26}$$

However, the mass indicated by the scale is not the real mass m. The mass indicated by the scale m_s is given as

$$m_s = -\frac{1}{g}F_s \tag{2.27}$$

where F_s is z-component of the total force acting to the system, i.e.

$$F_s = F_g + F_{cAO} + F_{cOW} + F_b. \tag{2.28}$$

Therefore the apparent flowrate reads

$$Q' = \frac{dm_s}{dt} = Q - \frac{1}{g}\frac{d}{dt}(F_{cAO} + F_{cOW} + F_b). \tag{2.29}$$

In the formula (2.29) we can recognize how the flowrate Q' computed directly from the scale indication differs from the real flowrate Q. Our task will be to compute this difference for the particular situations of our interest, e.g. for the pulsating flow.
We can also define apparent flowrates due to the capillary and buoyancy forces as

$$Q_{cAO} = -\frac{1}{g}\frac{d}{dt}F_{cAO}, \tag{2.30}$$

$$Q_{cOW} = -\frac{1}{g}\frac{d}{dt}F_{cOW}, \tag{2.31}$$

$$Q_b = -\frac{1}{g}\frac{d}{dt}F_b. \tag{2.32}$$

3 Numerical computations with MATLAB

3.1 Determining the coefficients c_{ij} and h_{0i}

In order to do the calculation we have to determine the coefficients (2.11) first. For computing the coefficients h_{01} and h_{02} we have to solve the equation (2.1) for a given volume V_0 and for given values of the equilibrium contact angles θ_{01} and θ_{02}. In the following calculation we will consider the following values of the parameters

$$V_{0OW} = 5000\,mm^3, \quad \cos\theta_{01OW} = -0.643, \quad \cos\theta_{02OW} = 0.707$$
$$V_{0AO} = 5785\,mm^3, \quad \cos\theta_{01AO} = 0.707, \quad \cos\theta_{02AO} = 0.707$$

corresponding to a volume of oil layer $V_O = 785\,mm^3$. The numerical solutions of equation (2.1) in MATLAB then give

$$h_{01OW} = 13.773\,mm, \quad h_{02OW} = 17.912\,mm$$
$$h_{01AO} = 18.546\,mm, \quad h_{02AO} = 19.453\,mm.$$

If we want to determine the parameters c_{ij} we have to solve the equation (2.1) for contact angles variating around their equilibrium values and look how the interface heights at the walls change and from this we can determine the derivatives. A computation in MATLAB gives

$$c_{11OW} = 1.1487\,mm, \quad c_{12OW} = -2.4854\,mm, \quad c_{21OW} = -0.0994\,mm, \quad c_{22OW} = 3.9603\,mm$$
$$c_{11AO} = 0.8372\,mm, \quad c_{12AO} = -0.5664\,mm, \quad c_{21AO} = -0.0227\,mm, \quad c_{22AO} = 1.8503\,mm.$$

In Fig. 3 – 6 below there are graphs of the functions $f(a, \cos\theta_1, \cos\theta_2, V_0)$ and $f(R, \cos\theta_1, \cos\theta_2, V_0)$ for both oil-water and air-oil interfaces for a given value of V_0. From the graphs we can see that the linear expansion considered in (2.12) is reasonable.

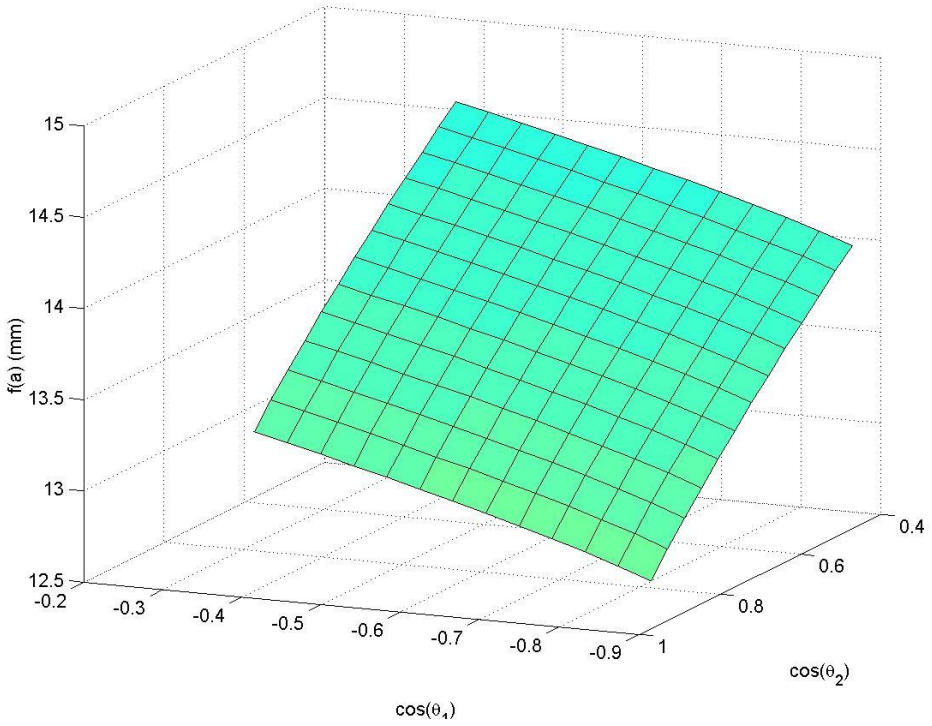

Fig. 3 Height of oil-water interface at tube wall as a function of contact angles for fixed volume

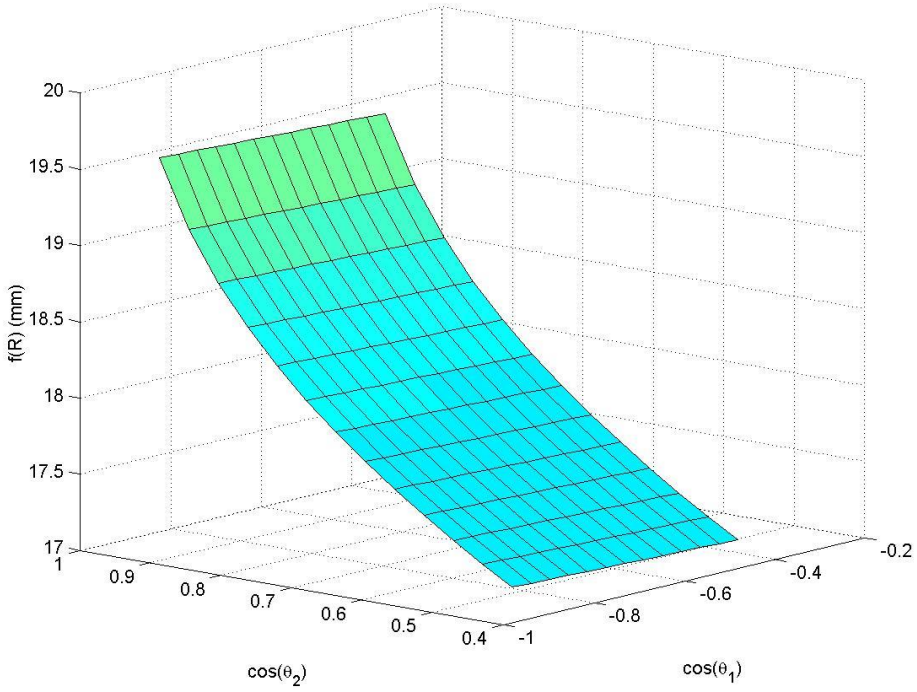

Fig. 4 Height of oil-water interface at beaker wall as a function of contact angles for fixed volume

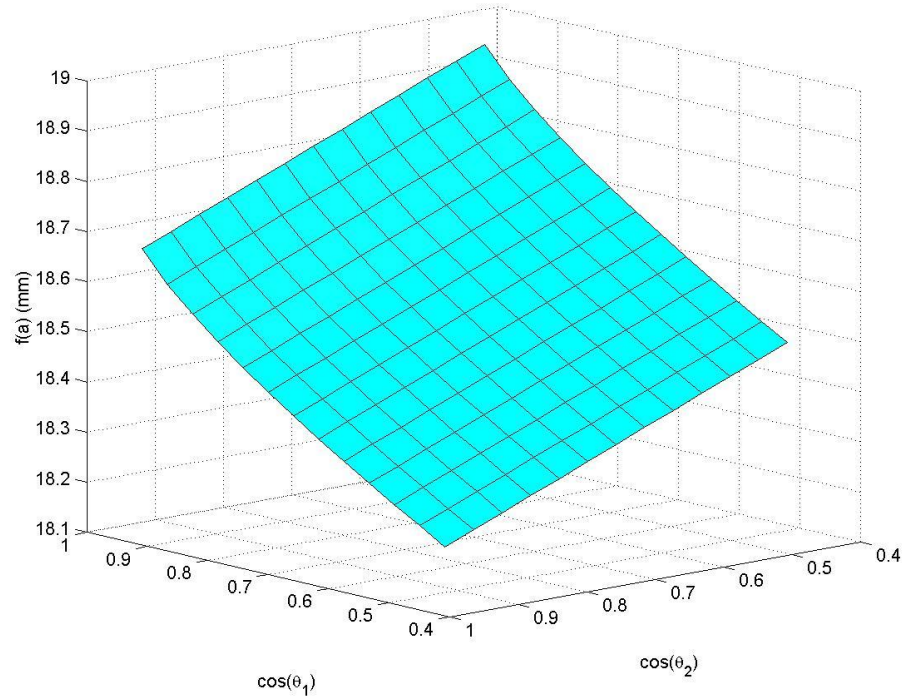

Fig. 5 Height of air-oil interface at tube wall as a function of contact angles for fixed volume

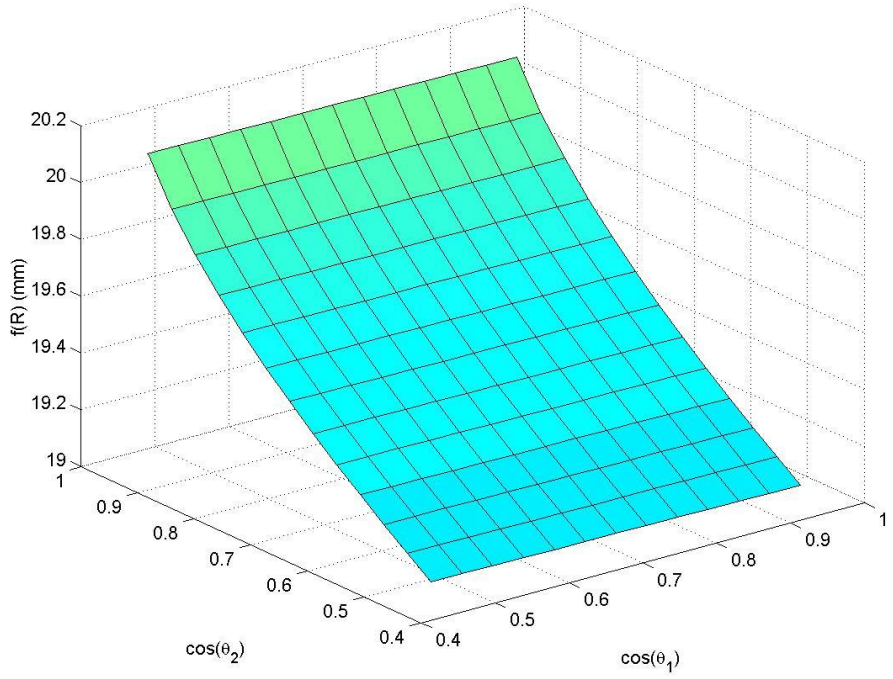

Fig. 6 Height of air-oil interface at beaker wall as a function of contact angles for fixed volume

3.2 Contact angle model for numerical computation

Before solving the differential equations (2.15) we need to specify the model of contact angle as a function of interface velocity.
Since we do not know the parameters of the Blake model we use the Seeberg model of contact angle.
For air-oil interface we need to know the dynamic viscosity of paraffin oil which is around 0.23 Pa.s, the surface tension of air-oil interface which is around 0.026 N/m and the equilibrium contact angles at the tube and at the wall which both are around 45°.
Since the Seeberg model is valid for liquid-air interface we have to make some assumptions for the water-oil interface. Since the viscosity of oil is much larger then viscosity of water we assume that the contact angle behaves like if there would be air instead of water. For the water-oil interface we therefore take the viscosity of oil in the Seeberg model and we take the value of surface tension of the water-oil interface of 0.041 N/m. Moreover we assume that for advancing contact angle starting from equilibrium value θ_0 the change of angle due to interface motion has just opposite sign as it would be for receding contact angle starting from equilibrium contact angle $90° - \theta_0$.
The value of equilibrium contact angle of the water-oil interface at the tube we consider to be 130° and at the wall we take 45°.
Example of dependency of change of cosine of contact angle with velocity of interface is in Fig.7. The figure depicts the Seeberg model curve and the Blake model for air-oil-tube interface. The parameters of the Blake curve were obtained by fitting to the Seeberg curve at velocity 0.89 μm/s which corresponds to a flowrate of 1 mL/h.

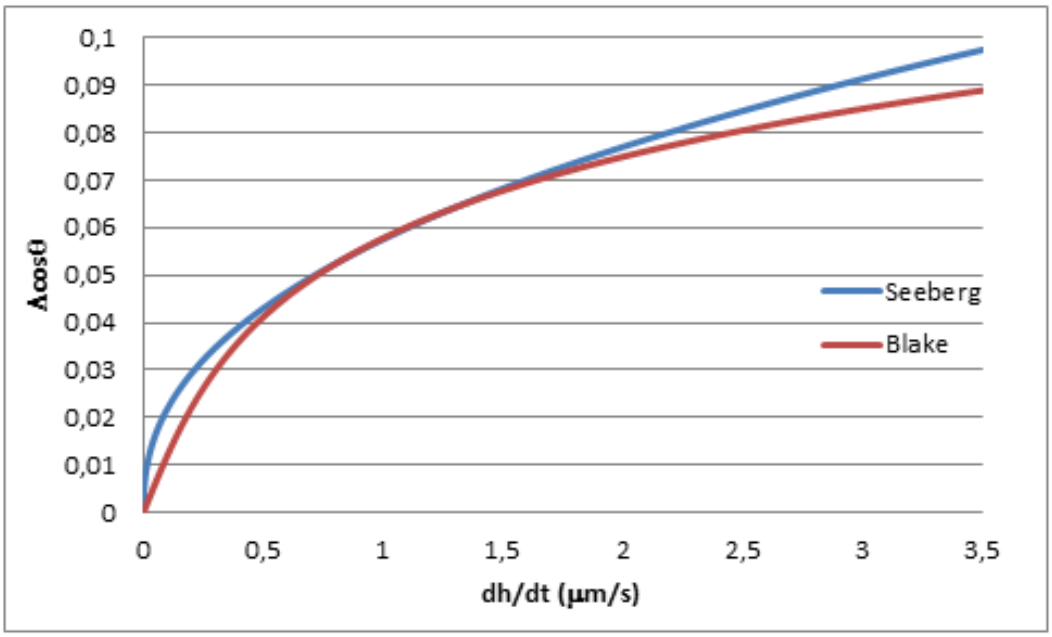

Fig. 7 Graphs of Seeberg and Blake model for air-oil-tube interface.

3.3 Stabilization of the measured flowrate

Before we proceed to the pulsating flow we will discuss certain properties of the solution which arise already for a constant flowrate and appear also for the pulsating flow.
When water starts to flow to the beaker, i.e. the flowrate is changed from zero value to some nonzero constant value, the contact angles of air-oil and water-oil interfaces with the tube start to evolve from their equilibrium values and it takes certain time before the contact angles stabilize at different values corresponding to certain velocity of the interfaces. During this process also the velocity of the interfaces evolve from zero value to certain stabilized value.
After the interface velocities and contact angles are stabilized the capillary forces acting between the interfaces and the tube are not changing anymore and they do not contribute to slope of the scale reading (they are just offset of the scale reading). At this stage the slope of the scale reading is shifted just by a contribution of buoyancy force which is growing with constant rate during the process.
It is necessary to know the stabilisation time since a calibration of a meter can start only after this time passes.

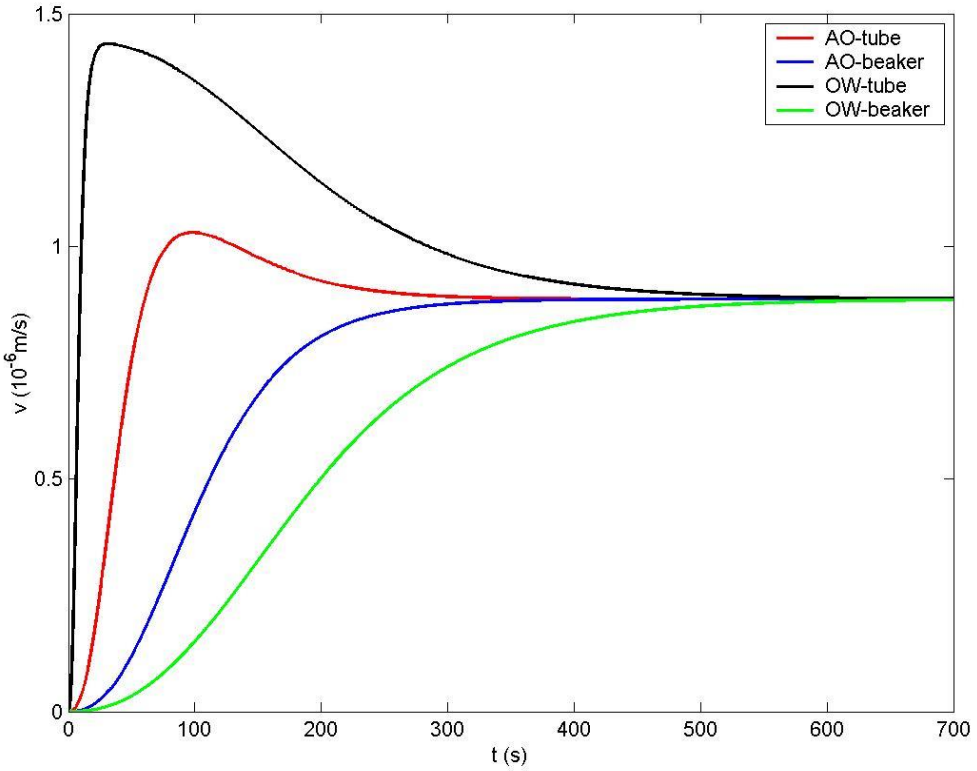

Fig.8 Evolution of velocity of interfaces for a flowrate of 1 mL/h.

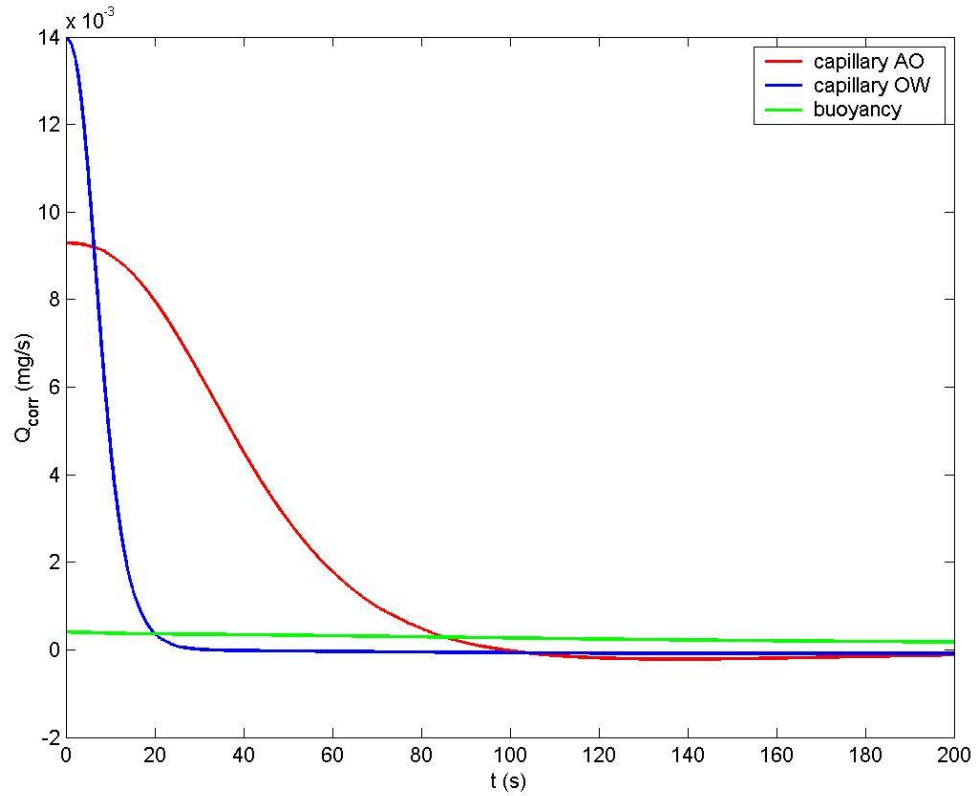

Fig.9 Evolution of apparent flowrate contributions caused by capillary and buoyancy forces for flowrate of 1 mL/h.

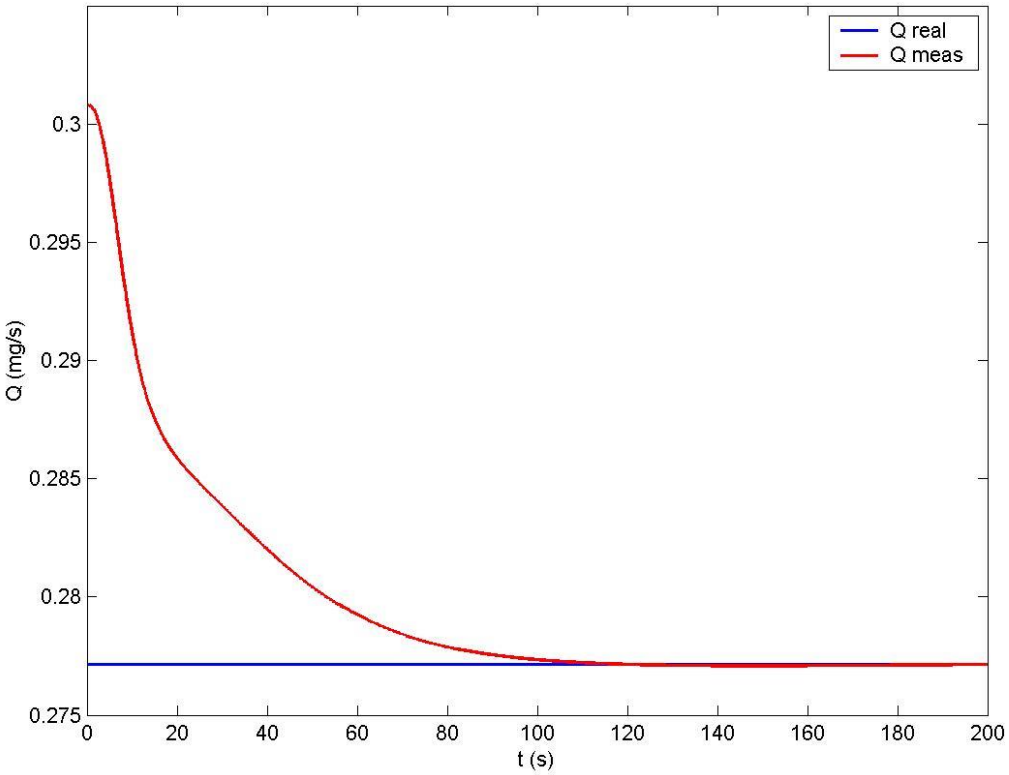

Fig.10 Evolution of the measured flowrate as compared to the real value of flowrate which in this case is 1 mL/h corresponding to 0.277 mg/s for density of 997 kg/m^3.

Evolution of velocity of all interfaces for flowrate of 1 mL/h is depicted in Fig. 8. We see that after some time all velocities tend to certain value which is for all interfaces the same. This value corresponds to a velocity of surface in stage when the surface shape is not changing anymore.
Evolution of contributions of capillary forces and buoyancy force to the measured flowrate for real flowrate 1 mL/h is depicted in Fig. 9. We see that the capillary contribution tends to zero after some time which corresponds to the stabilized contact angles. The buoyancy contribution tends to certain nonzero value.
Evolution of the measured flowrate as compared to the real flowrate of 1 mL/h is depicted in Fig. 10.
For flowrates others then 1 mL/h the curves look qualitatively the same just in different scales.

Now we will express the stabilisation times quantitatively. The measured flowrate converges to certain value which we will denote Q'_s. We consider the measured flowrate as stabilized if its value does not differ from Q'_s by more than 0.1 %. The stabilization time is then the time needed to obtain the stabilized flowrate, i.e. the stabilisation time t_s is the smallest time such that for $t \geq t_s$ we have

$$\delta_Q = \frac{Q' - Q'_s}{Q'_s} . 100 \leq 0.1 \quad . \tag{3.3.1}$$

The value of 0.1 % was chosen to be an order of magnitude smaller than the expected uncertainty of a flow measurement.
The converged value Q'_s is given by the real flowrate corrected by the buoyancy contribution. The capillary forces do not contribute to the converged flowrate since they do not change at this stage. Therefore we have

$$Q_s{}' = \frac{dm}{dt} - \frac{1}{g}\frac{dF_b}{dt} \tag{3.3.2}$$

where F_b is given by (2.20). In the formula (2.20) the pressure jumps also do not change with time as well as the thickness of the oil layer. Since the interface shapes are not changing at this stage the velocity of the interfaces is given just by a ratio of volume flowrate and area of the open surface. In terms of the real mass flowrate Q we can write

$$\frac{dh}{dt} = \frac{Q}{\rho_W \pi (R^2 - a^2)}. \tag{3.3.3}$$

Using these formulas we arrive to the following expression for the converged measured flowrate

$$Q_s{}' = Q\left(1 - \frac{\rho_A}{\rho_W}\right)\left(1 + \frac{a^2}{R^2 - a^2}\right). \tag{3.3.4}$$

Now we want to find the time when the measured flowrate starts to differ from the flowrate given by (3.3.4) only by 0.1 %. These times have been determined numerically for various flowrates and are summarised in Tab. 1.

Q_V (mL/h)	0.001	0.01	0.1	1	10
t_s (s)	4906	1290	339	89.3	23.5

Tab. 1 Stabilisation times for various flowrates.

3.4 Scaling of the solutions

We can even derive a formula describing how the stabilisation time depends on flowrate. The derivation is based on scaling properties of solutions of the equations (2.15) with the Seeberg model of dynamic contact angle (2.17). More generally we can consider the differential equations (2.15) with a model of dynamic contact angle similar to the Seeberg one but with general constants α, β, ω

$$\Delta(\dot{h}) = -\ \alpha(\beta \dot{h})^{\omega} \quad . \tag{3.4.1}$$

First we will prove the following lemma.

Lemma 1. Let $h_{1i}(t), h_{2i}(t)$ be a solution of system of equations (2.15) with Δ function given by (3.4.1), with certain volume growth function $V(t) = V_i(t)$ and with initial conditions $h_{1i}(0) = 0, h_{2i}(0) = 0$ (we drop bars above h here). Then functions $h_{1\lambda}(t)$, $h_{2\lambda}(t)$ related to the functions $h_{1i}(t), h_{2i}(t)$ as

$$\begin{aligned} h_{1\lambda}(t) &= \lambda^{\omega} h_{1i}(\lambda^{1-\omega} t) \\ h_{2\lambda}(t) &= \lambda^{\omega} h_{2i}(\lambda^{1-\omega} t) \end{aligned} \tag{3.4.2}$$

where λ is a constant are solution of the system (2.15) with Δ function given by (3.4.1), with volume growth function

$$V(t) = \lambda^{\omega} V_i(\lambda^{1-\omega} t) \tag{3.4.3}$$

and initial conditions $h_{1\lambda}(0) = 0,\ h_{2\lambda}(0) = 0$.

Proof. The system of differential equations (2.15) with the model of dynamic contact angle (3.4.1) can be written as (we drop the bars above h)

$$-\alpha_1\left(\beta_1\frac{dh_1}{dt}\right)^{\omega}=\frac{1}{c_{11}c_{22}-c_{12}c_{21}}\left(c_{22}h_1(t)-c_{12}h_2(t)-(c_{22}-c_{12})\,V(t)/S\right)$$

$$-\alpha_2\left(\beta_2\frac{dh_2}{dt}\right)^{\omega}=\frac{-1}{c_{11}c_{22}-c_{12}c_{21}}\left(c_{21}h_1(t)-c_{11}h_2(t)-(c_{21}-c_{11})\,V(t)/S\right).$$

To show that functions $h_{1\lambda}(t)$, $h_{2\lambda}(t)$ given by (3.4.2) are a solution of this system we insert these functions and (3.4.3) into these equations. We denote $\tau=\lambda^{1-\omega}t$. Thus we obtain

$$-\alpha_1\left(\beta_1\lambda^{\omega}\frac{dh_{1i}}{d\tau}\frac{d\tau}{dt}\right)^{\omega}=\frac{1}{c_{11}c_{22}-c_{12}c_{21}}\lambda^{\omega}\left(c_{22}h_{1i}(\tau)-c_{12}h_{2i}(\tau)-(c_{22}-c_{12})\,V_i(\tau)/S\right)$$

$$-\alpha_2\left(\beta_2\lambda^{\omega}\frac{dh_{2i}}{d\tau}\frac{d\tau}{dt}\right)^{\omega}=\frac{-1}{c_{11}c_{22}-c_{12}c_{21}}\lambda^{\omega}\left(c_{21}h_{1i}(\tau)-c_{11}h_{2i}(\tau)-(c_{21}-c_{11})\,V_i(\tau)/S\right).$$

This leads to

$$-\alpha_1\left(\beta_1\frac{dh_{1i}}{d\tau}\right)^{\omega}=\frac{1}{c_{11}c_{22}-c_{12}c_{21}}\left(c_{22}h_{1i}(\tau)-c_{12}h_{2i}(\tau)-(c_{22}-c_{12})\,V_i(\tau)/S\right)$$

$$-\alpha_2\left(\beta_2\frac{dh_{2i}}{d\tau}\right)^{\omega}=\frac{-1}{c_{11}c_{22}-c_{12}c_{21}}\left(c_{21}h_{1i}(\tau)-c_{11}h_{2i}(\tau)-(c_{21}-c_{11})\,V_i(\tau)/S\right).$$

This already proves the lemma since we supposed that $h_{1i}(t), h_{2i}(t)$ is solution of the system with $V(t)=V_i(t)$. ■

Now let us check how the real and measured flowrate change after transformation (3.4.2), (3.4.3). For the real volumetric flowrate we just need to do a time derivative of the formula (3.4.3). We obtain

$$Q_{V\lambda}(t)=\frac{d}{dt}\lambda^{\omega}V_i(\lambda^{1-\omega}t)=\lambda^{\omega}\frac{d}{d\tau}V_i(\lambda^{1-\omega}t)\frac{d\tau}{dt}=\lambda Q_{Vi}(\lambda^{1-\omega}t)\ . \tag{3.4.4}$$

For the real mass flowrate we just multiply this equation by water density and therefore we obtain the same transformation formula

$$Q_{\lambda}(t)=\lambda Q_i(\lambda^{1-\omega}t)\ . \tag{3.4.5}$$

The difference between measured and real flowrate is given by the time derivatives of the buoyancy force and the capillary forces (see (2.29)). The buoyancy force is given by (2.20) and the capillary forces are given by (2.19). We see that these forces are given as linear combinations of the volume growth function $V(t)$ and the interface height functions $h_{1OW}(t), h_{1AO}(t), h_{2OW}(t), h_{2AO}(t)$. The transformation formula of the interface height functions (3.4.2) is the same as the transformation formula for volume growth function (3.4.3). Therefore, also the time derivative of the interface height functions transforms according to the same formula as the time derivative of the volume growth function or in other words according to the same formula as volumetric flowrate (3.4.4) (or mass flowrate (3.4.5)).
Therefore the apparent flowrates given by capillary and buoyancy forces (2.30), (2.31), (2.32) transforms according to the same formula as the real mass flowrate (3.4.5). And, therefore, also the measured mass flowrate transforms according to the same formula. The transformation reads

$$Q'_{\lambda}(t)=\lambda Q'_i(\lambda^{1-\omega}t)\ . \tag{3.4.6}$$

Now we can use the *lemma 1* to obtain some information on how stabilisation times change with flowrate. In case of a constant real flowrate the measured flowrate converges to certain value with increasing time as we already discussed. This value can be given as

$$Q'_s = \lim_{t\to\infty} Q'(t)\,. \tag{3.4.7}$$

Under the transformation (3.4.6) this value transforms as

$$Q'_{s\lambda} = \lambda Q'_{si}\ . \tag{3.4.8}$$

The relative deviation of instantaneous measured flowrate from the converged flowrate given by (3.3.1) transforms as follows

$$\delta_{Q\lambda}(t) = \frac{Q'_\lambda(t)\ - Q'_{s\lambda}}{Q'_{s\lambda}}.100 = \frac{Q'_i(\lambda^{1-\omega}t)\ - Q'_{si}}{Q'_{si}}.100 = \delta_{Qi}(\lambda^{1-\omega}t)\ . \tag{3.4.9}$$

Transformation of the stabilization time follows from the following equation

$$\delta_{Q\lambda}(t_{s\lambda}) = \delta_{Qi}(t_{si})\ . \tag{3.4.10}$$

Using (3.4.9) we obtain

$$\delta_{Q\lambda}(t_{s\lambda}) = \delta_{Qi}(\lambda^{1-\omega}t_{s\lambda}) = \delta_{Qi}(t_{si}) \tag{3.4.11}$$

and therefore

$$t_{s\lambda} = \lambda^{\omega-1}t_{si}\ . \tag{3.4.12}$$

We consider a constant real flowrate. According to (3.4.5) this flowrate transforms

$$Q_\lambda = \lambda Q_i \tag{3.4.13}$$

and therefore λ can be written as

$$\lambda = \frac{Q_\lambda}{Q_i}\ . \tag{3.4.14}$$

Inserting this into (3.4.12) we obtain the resulting formula

$$t_{s\lambda} = \left(\frac{Q_\lambda}{Q_i}\right)^{\omega-1} t_{si}\ . \tag{3.4.15}$$

We can check the formula and compare its predictions with the predictions of the numerical model. For the Seeberg model we have $\omega = 0.42$. Therefore if the flowrate is increased by a factor of 10 the stabilization time decreases by a factor of $10^{-0.58}$ (= 0.263). This is also the case of numerical results summarized in Tab. 1.

3.5 Pulsating flow

3.5.1 Types of oscillations considered

The flowrate oscillations are characterised by three parameters – the average volumetric flowrate Q_0, the relative flowrate amplitude A_r and flowrate period T. The oscillations can have various shapes. In this report we investigate two shapes – sinusoidal and triangular.
In case of sinusoidal pulsations the volumetric flowrate depends on time in the following way

$$Q_V(t) = Q_0\left(1 + A_r \cos\left(\frac{2\pi t}{T}\right)\right). \tag{3.5.1}$$

For the volume increase in case of the sinusoidal oscillations we obtain

$$V(t) = \int_0^t Q_V(t)\,dt = Q_0\left(t + \frac{T}{2\pi}A_r \sin\left(\frac{2\pi t}{T}\right)\right). \tag{3.5.2}$$

In case of triangular pulsations the volumetric flowrate depends on time in the following way

$$Q_V(t) = Q_0\left(1 + A_r \frac{(-1)^{\mathrm{fix}\left(\frac{2t}{T}\right)}}{\frac{T}{4}}\left(\mathrm{mod}\left(t, \frac{T}{2}\right) - \frac{T}{4}\right)\right) \tag{3.5.3}$$

where the function "fix(x)" gives a whole part of the number "x" and the function "mod(x, y)" gives a remainder after dividing of "x" by "y".
For the volume increase in case of the triangular oscillations we obtain

$$V(t) = \int_0^t Q_V(t)\,dt = Q_0\left(t - A_r(-1)^{\mathrm{fix}\left(\frac{2t}{T}\right)}\mathrm{mod}\left(t, \frac{T}{2}\right).\left(1 - \frac{2}{T}.\mathrm{mod}\left(t, \frac{T}{2}\right)\right)\right). \tag{3.5.4}$$

The aim of the simulation is to compute the apparent flowrate (2.29) as a function of time and to compare it with the real flowrate. Namely we are interested in comparison of the oscillation parameters A_r and T.

3.5.2 Results

The simulations have been done for a fixed value of the period $T = 5\,s$, five values of the relative amplitude $A_r = 0.1; 0.3; 0.5; 0.7; 0.9$ and for five values of the average volumetric flowrate $Q_0 = (0.001; 0.01; 0.1; 1; 10)$ mL/h . The results for different values of the period T can be obtained using the scaling properties of the solution again as we will see later.
The figures 11 – 22 show oscillations of the real flowrate, the measured flowrate (2.29) and the components of deviation of the measured flowrate from the real flowrate caused by the capillary and buoyancy forces (2.30), (2.31), (2.32) for various parameters of the oscillating flow. These results are discussed in the next section.

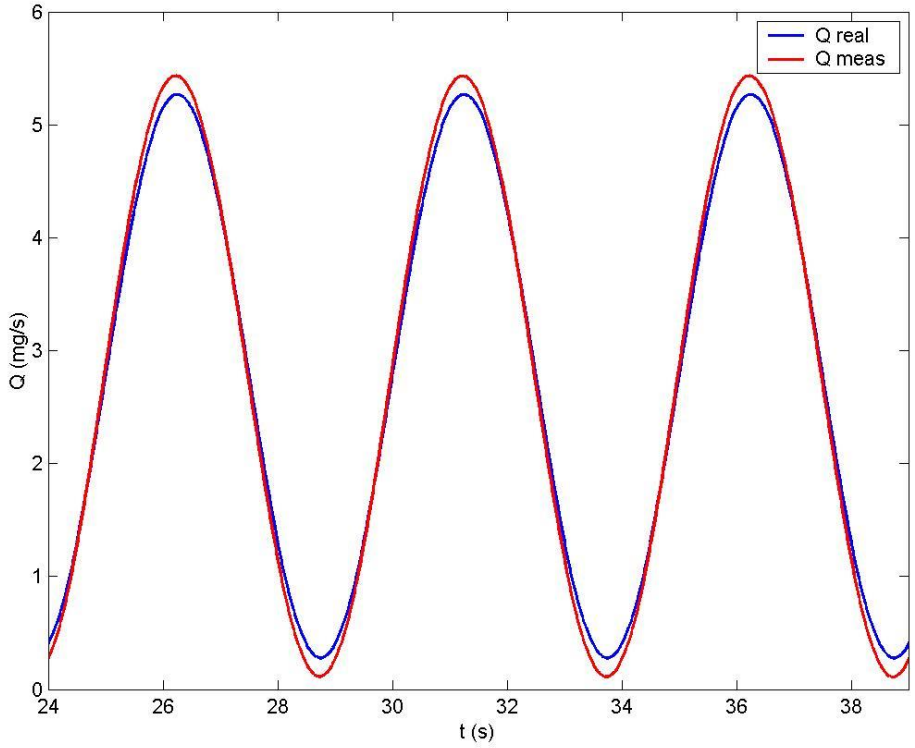

Fig. 11 Real and measured (apparent) flowrate for $Q_0 = 10\ mL/h$ and $A_r = 0.9$, sinusoidal oscillations

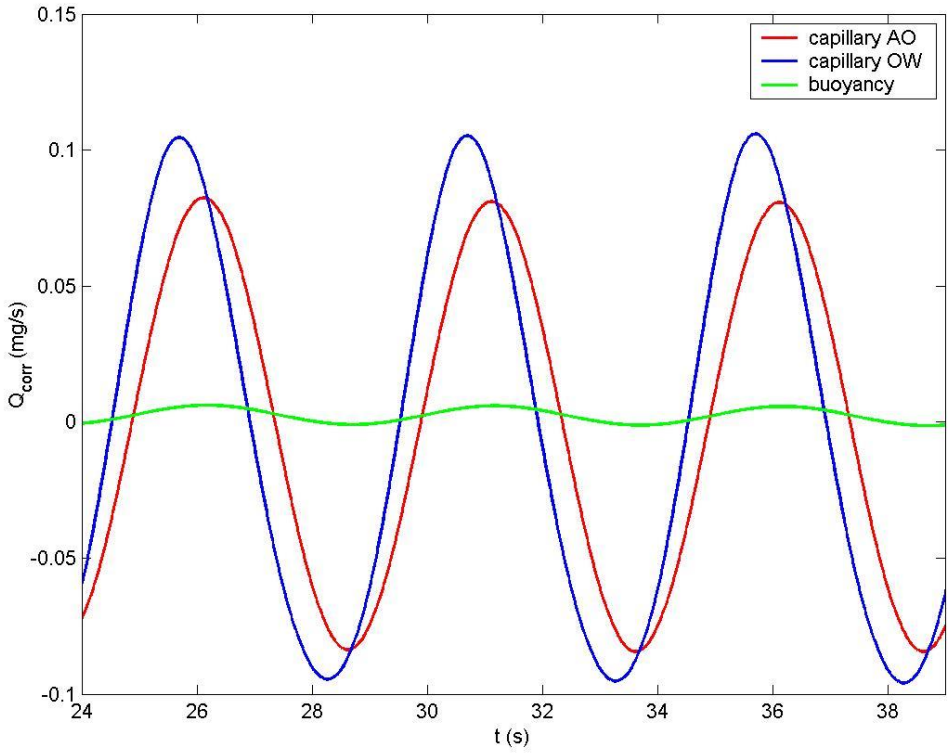

Fig. 12 Contributions to apparent flowrate for $Q_0 = 10\ mL/h$ and $A_r = 0.9$, sinusoidal oscillations

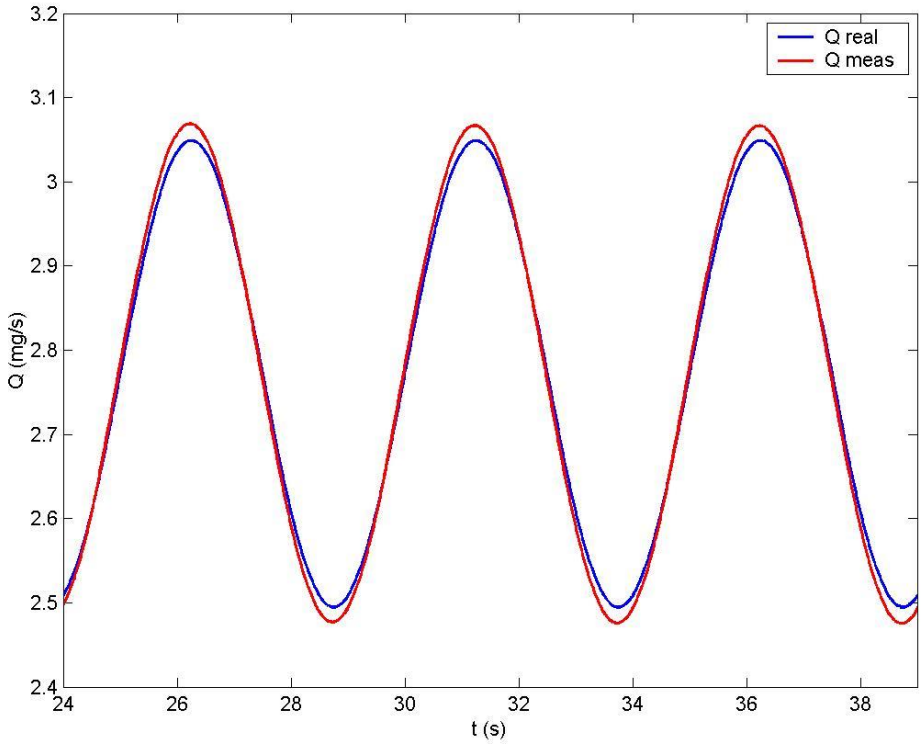

Fig. 13 Real and measured (apparent) flowrate for $Q_0 = 10\ mL/h$ and $A_r = 0.1$, sinusoidal oscillations

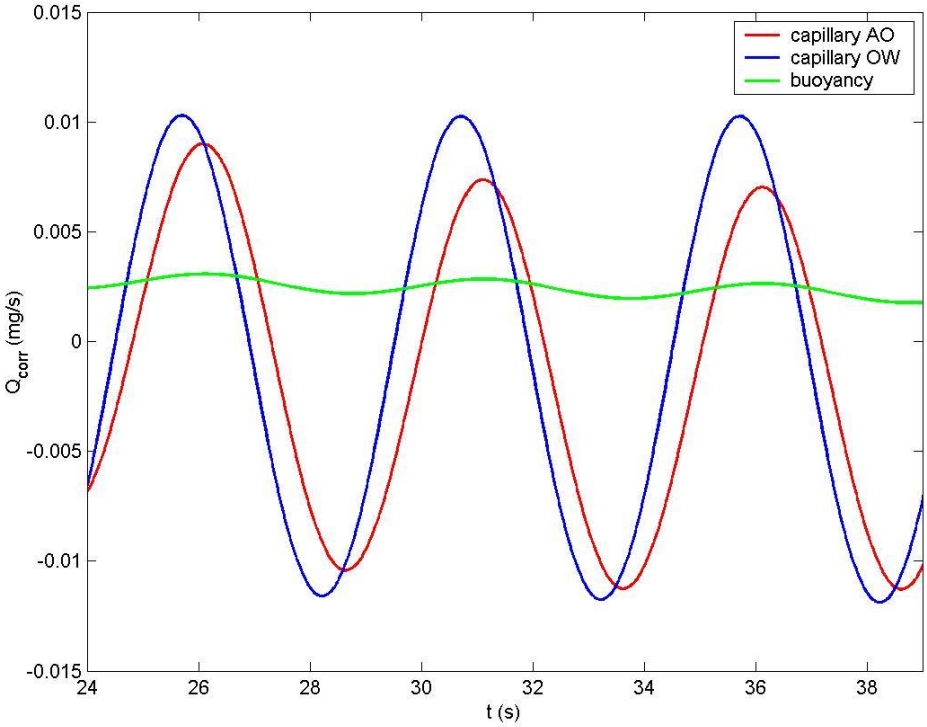

Fig. 14 Contributions to apparent flowrate for $Q_0 = 10\ mL/h$ and $A_r = 0.1$, sinusoidal oscillations

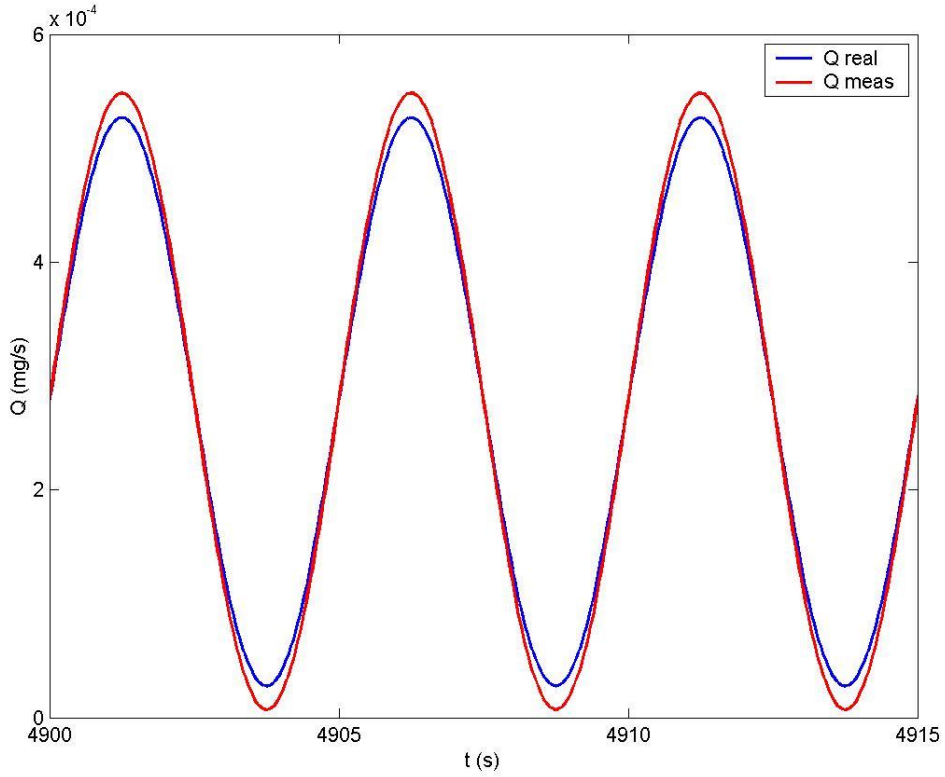

Fig. 15 Real and measured (apparent) flowrate for $Q_0 = 0.001\ mL/h$ and $A_r = 0.9$, sinusoidal oscillations

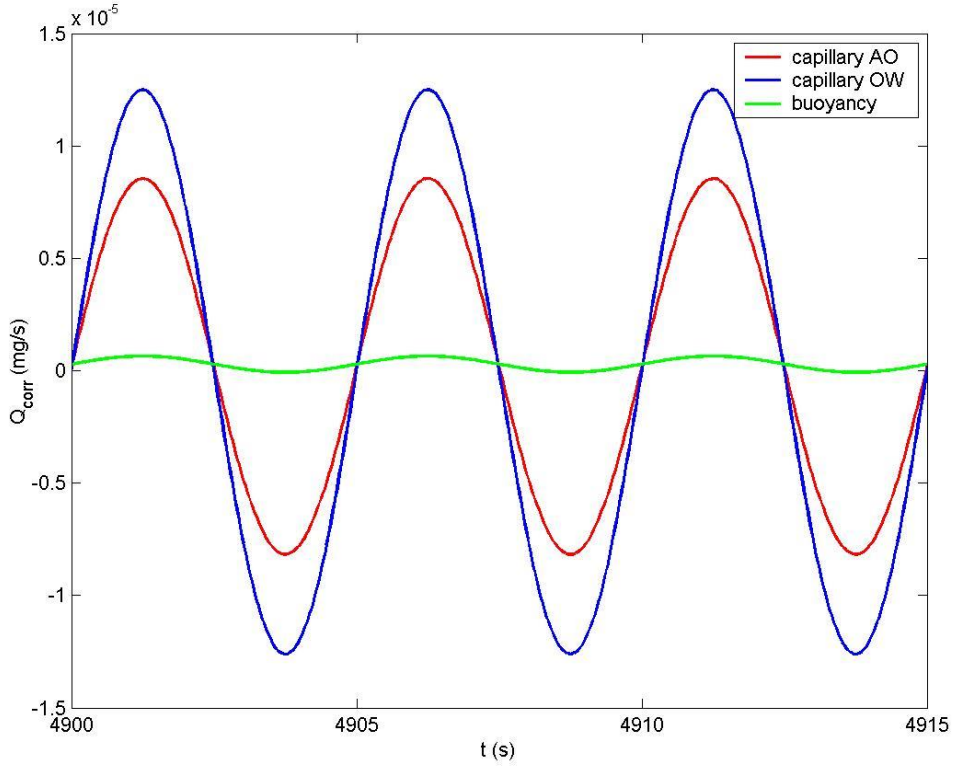

Fig. 16 Contributions to apparent flowrate for $Q_0 = 0.001\ mL/h$ and $A_r = 0.9$, sinusoidal oscillations

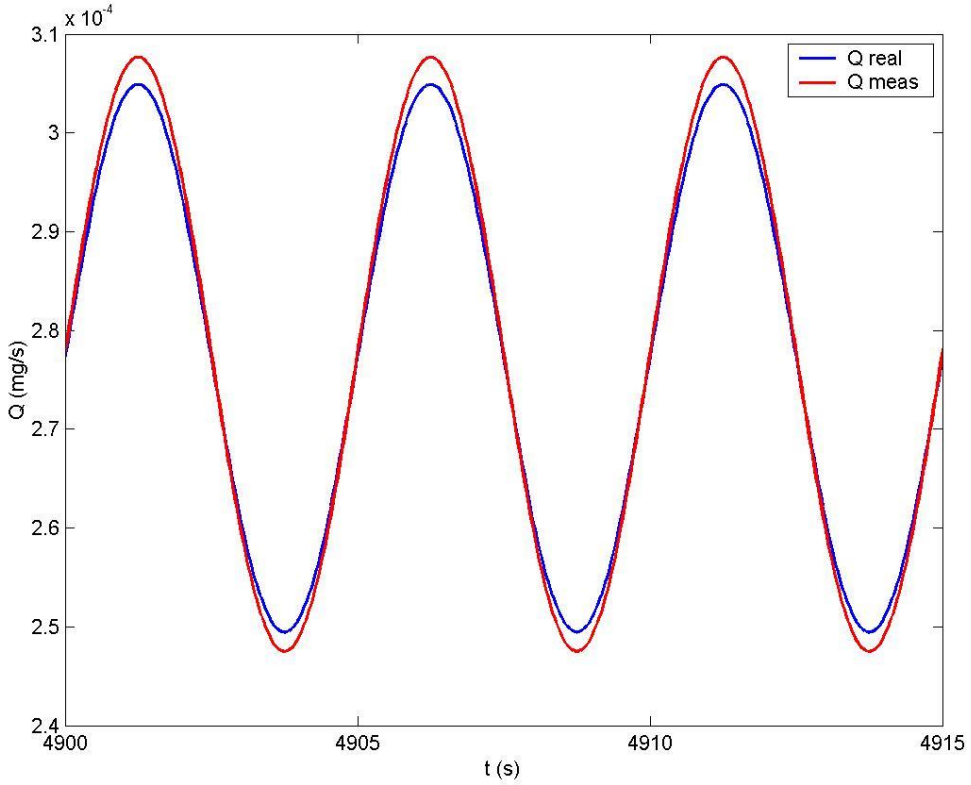

Fig. 17 Real and measured (apparent) flowrate for $Q_0 = 0.001\ mL/h$ and $A_r = 0.1$, sinusoidal oscillations

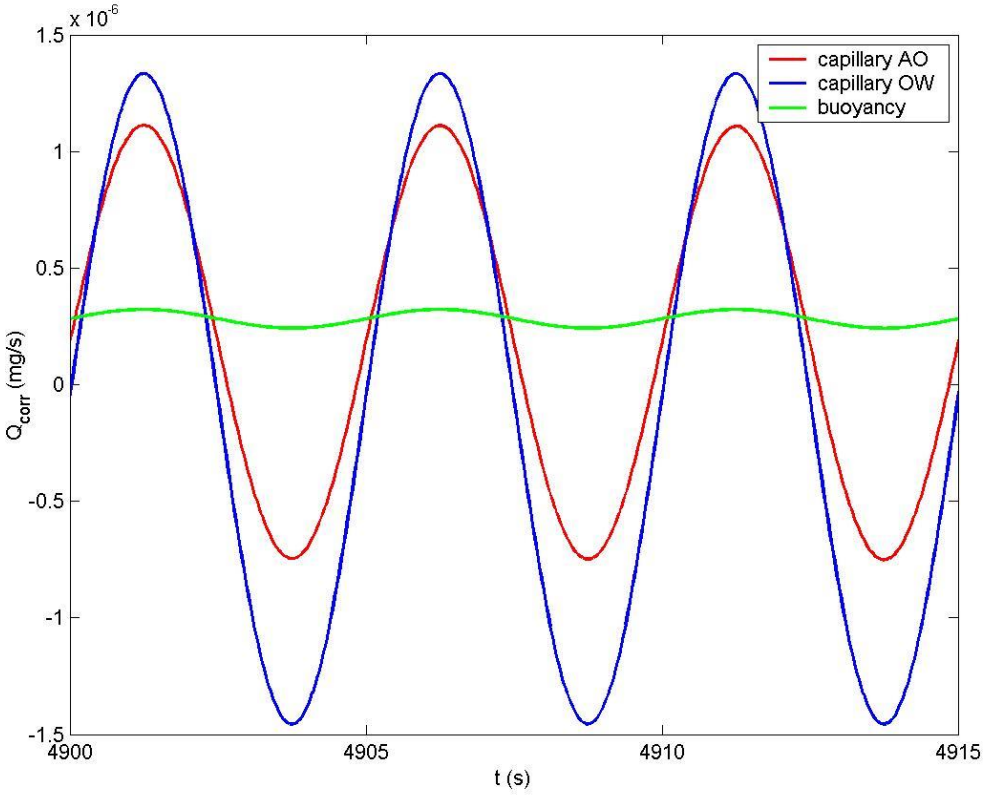

Fig. 18 Contributions to apparent flowrate for $Q_0 = 0.001\ mL/h$ and $A_r = 0.1$, sinusoidal oscillations

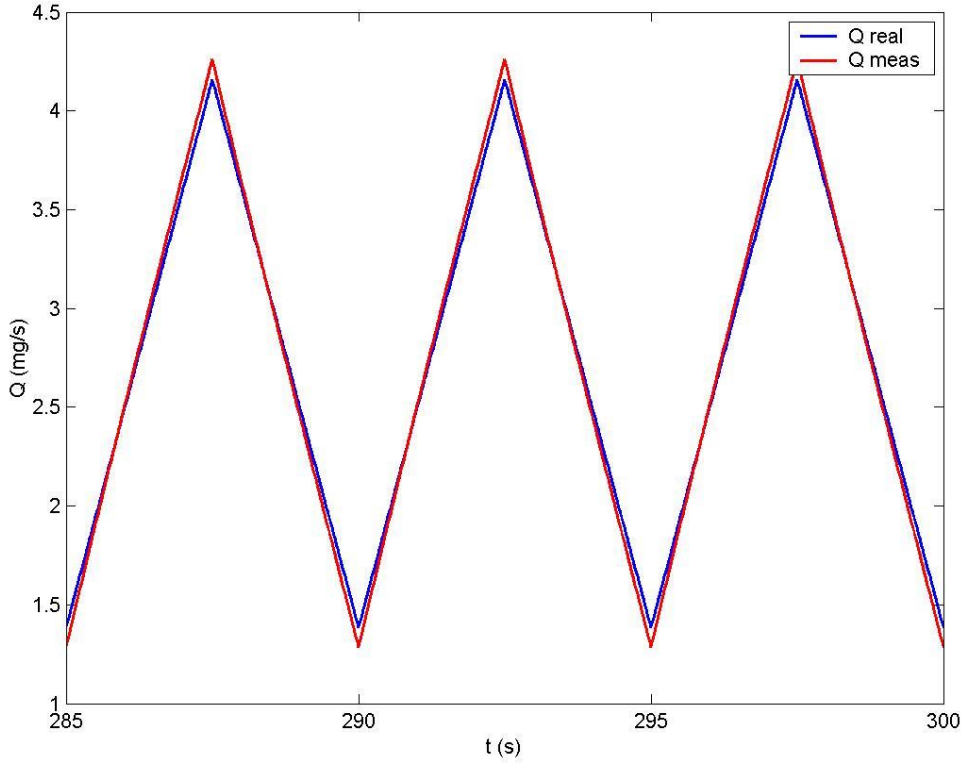

Fig. 19 Real and measured (apparent) flowrate for $Q_0 = 10\ mL/h$ and $A_r = 0.5$, triangular oscillations

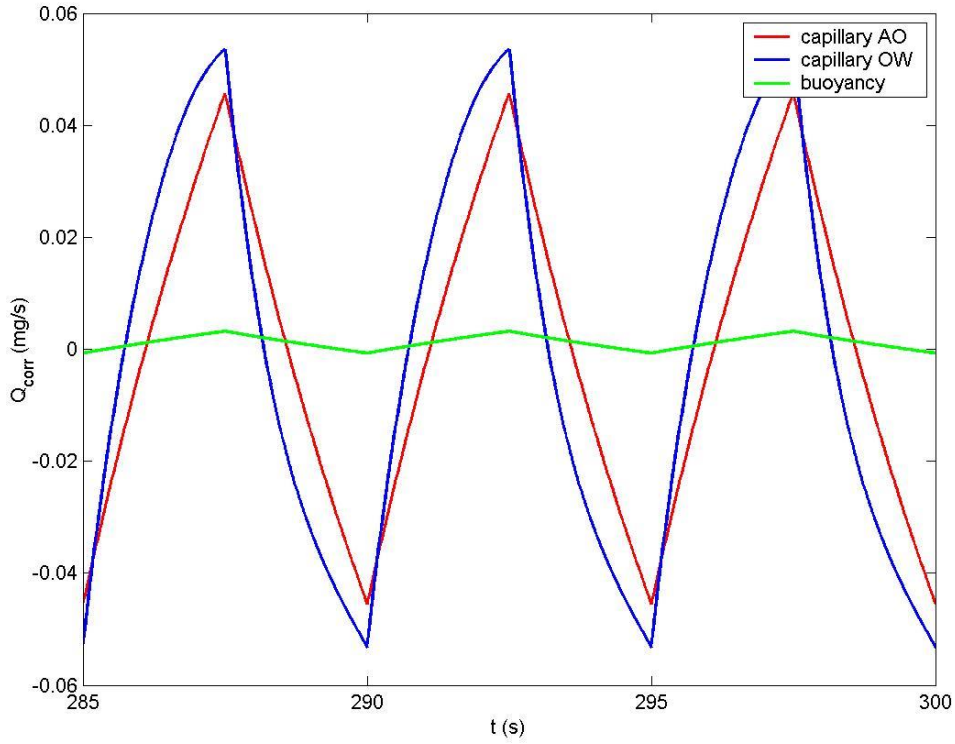

Fig. 20 Contributions to apparent flowrate for $Q_0 = 10\ mL/h$ and $A_r = 0.5$, triangular oscillations

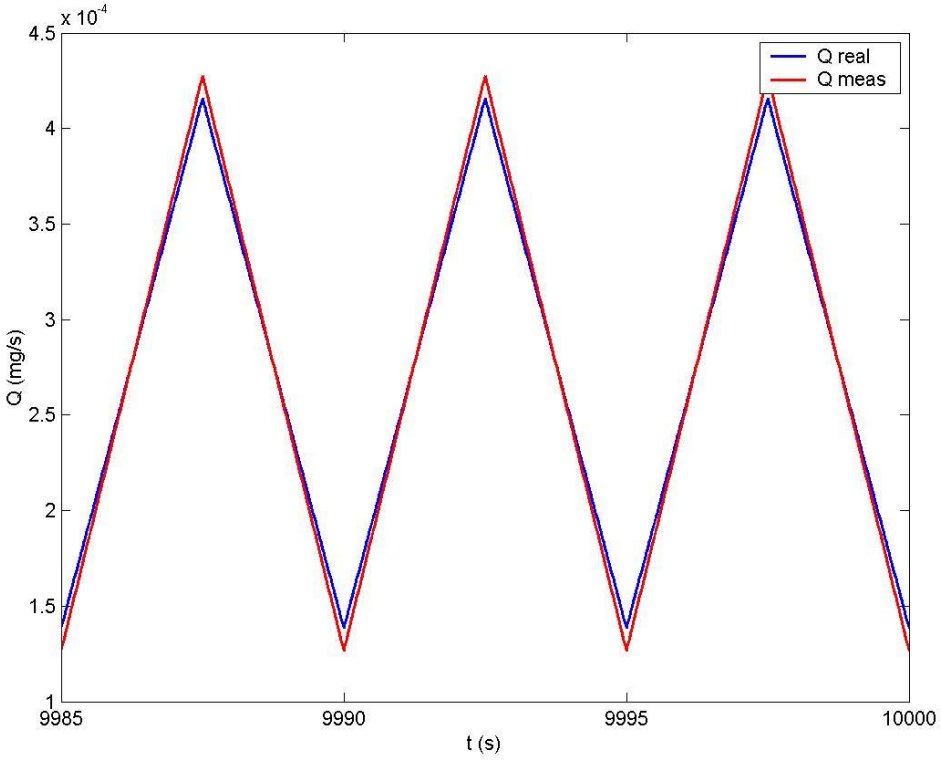

Fig. 21 Real and measured (apparent) flowrate for $Q_0 = 0.001\ mL/h$ and $A_r = 0.5$, triangular oscillations

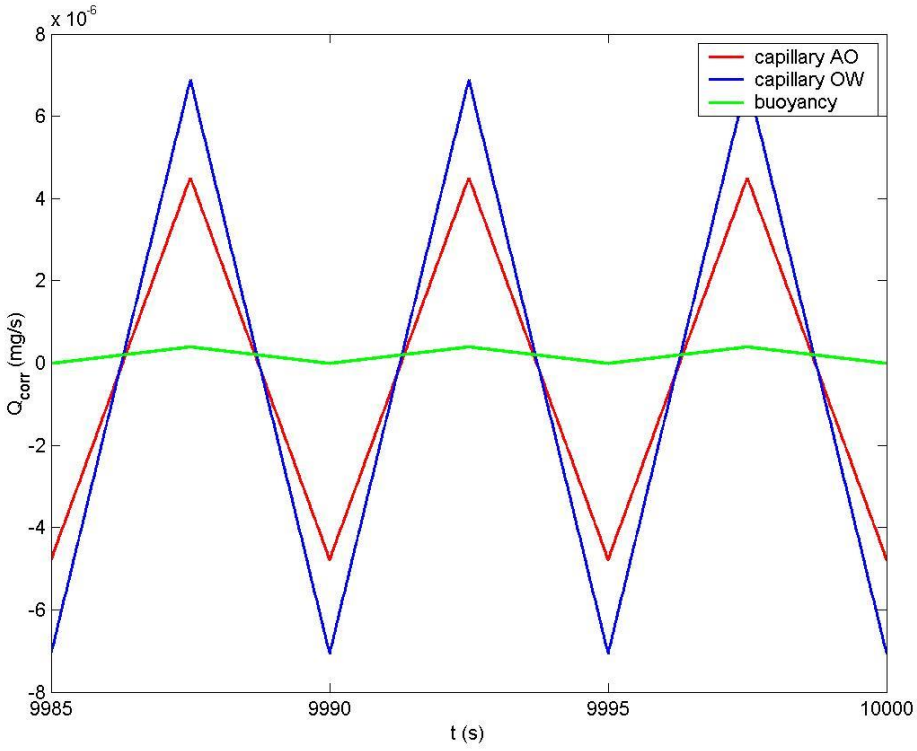

Fig. 22 Contributions to apparent flowrate for $Q_0 = 0.001\ mL/h$ and $A_r = 0.5$, triangular oscillations

3.5.3 Discussion of the simulation results

The simulation results show that the real and measured period of oscillations are equal, i.e. $T' = T$. From Fig. 13 and 14 we can see that certain phase shift can occur.
Value of the mean real flowrate differs from the value of mean apparent flowrate, e.g. because of the buoyancy. This we have already seen for the stationary case. The contribution of buoyancy to the apparent flowrate can be seen clearly e.g. in Fig. 14 and 18.
The value of relative amplitude of the measured flowrate is larger than the value for real flowrate. We will look to this difference in more detail.
We determine the relative amplitude of the apparent (measured) flowrate (2.29) according to the formula

$$A'_r = \frac{Q'_{max} - Q'_{min}}{Q'_{max} + Q'_{min}} \tag{3.5.5}$$

where Q'_{max} is a local maximum of the oscillating apparent flowrate and Q'_{min} is a local minimum of the oscillating apparent flowrate. Then we define a deviation of the apparent relative amplitude from the real relative amplitude as

$$\delta_A = \frac{A'_r - A_r}{A_r}.100 \ . \tag{3.5.6}$$

The following tables summarize the values of δ_A obtained from numerical simulations for various parameters of the oscillating flow.

	$Q_0 =$ $0.001\ mL/h$	$Q_0 =$ $0.01\ mL/h$	$Q_0 =$ $0.1\ mL/h$	$Q_0 =$ $1\ mL/h$	$Q_0 =$ $10\ mL/h$
A_r	$\delta_A(\%)$				
0.1	8.50	8.50	8.50	8.30	7.00
0.3	8.53	8.47	8.47	8.33	7.00
0.5	8.54	8.48	8.46	8.34	7.00
0.7	8.54	8.47	8.46	8.33	7.00
0.9	8.53	8.48	8.46	8.31	7.00

Tab. 2 Values of δ_A for sinusoidal oscillations and $T = 5\ s$

	$Q_0 =$ $0.001\ mL/h$	$Q_0 =$ $0.01\ mL/h$	$Q_0 =$ $0.1\ mL/h$	$Q_0 =$ $1\ mL/h$	$Q_0 =$ $10\ mL/h$
A_r	$\delta_A(\%)$				
0.1	8.50	8.50	8.50	8.40	7.20
0.3	8.53	8.50	8.47	8.37	7.23
0.5	8.54	8.48	8.48	8.36	7.22
0.7	8.54	8.49	8.47	8.36	7.23
0.9	8.54	8.49	8.48	8.34	7.23

Tab. 3 Values of δ_A for triangular oscillations and $T = 5\ s$

Values of δ_A for period different from 5 s can be obtained from the scaling properties described in lemma 1. The transformation of volume increase function (3.4.3) can be in case of the oscillating flow achieved by the following transformation of parameters Q_0 and T

$$Q_{0\lambda} = \lambda Q_{0i} \ , \tag{3.5.7}$$

$$T_\lambda = \lambda^{\omega-1} T_i \ . \tag{3.5.8}$$

This transformation of parameters leads to a change of the real and the apparent flowrates described by formulas (3.4.5) and (3.4.6). The value of apparent relative amplitude (3.5.5) as well as the value of real relative amplitude remains unchanged after this transformation and therefore also the value of δ_A remains unchanged. Therefore we have

$$\delta_A(A_r,\ Q_{0\lambda},\ T_\lambda) = \delta_A(A_r, Q_{0i}, T_i) \ . \tag{3.5.9}$$

Eliminating the parameter λ from equations (3.5.7) and (3.5.8) we obtain

$$Q_{0i} = Q_{0\lambda} \left(\frac{T_\lambda}{T_i}\right)^{\frac{1}{1-\omega}} \ . \tag{3.5.10}$$

Inserting this into (3.5.9) we obtain

$$\delta_A(A_r,\ Q_{0\lambda},\ T_\lambda) = \delta_A\left(A_r,\ Q_{0\lambda}\left(\frac{T_\lambda}{T_i}\right)^{\frac{1}{1-\omega}}, T_i\right) \ . \tag{3.5.11}$$

This equation says that the value of δ_A for a set of flow parameters $A_r,\ Q_0 = Q_{0\lambda},\ T = T_\lambda$ is the same as the value of δ_A for period $T = T_i$ which we can choose to be $T_i = 5\ s$, mean real flowrate $Q_0 = Q_{0\lambda} \cdot (T_\lambda/T_i)^{1/(1-\omega)}$ and unchanged value of A_r. Therefore, this formula allows us to get the values of δ_A for periods which differ from 5 s. Since the δ_A does not change much with Q_0 it will not change much with T too.

We can conclude that for $T = 5\ s$ the difference of relative amplitude of the measured flowrate from the real flowrate is between 7 % and 8.6 % for the considered ranges of parameters Q_0, A_r. For different value of T this shift will not be much different.

4 Conclusions

A physical model of non-stationary interaction of the tube inserted into the beaker with the fluids in the beaker was developed for gravimetric nano-flow facility of DTI with special emphasis on the capillary and buoyancy forces. The model is based on equation for the shape of interfaces between different fluids in the beaker (air-oil and oil-water) and on models of contact angles between these interfaces and the tube and beaker wall. In these models a dynamical contact angle is considered which can change with motion of the interfaces and which depends on velocity of the interfaces.
The influence of fluid streams in neighbourhood of the interfaces on the shape of the interfaces was not considered in this work since the velocities are so small that this effect is probably negligible.

This physical model was implemented into MATLAB and the equations of this model were solved numerically first for the case of stationary flow and then for the case of pulsating flow.

In case of stationary flow the stabilisation time of the system was investigated. It was shown that according to the model it takes some time before the measured flowrate reaches a stable non-changing value. At the beginning of a measurement when a constant real flowrate starts to flow the measured flowrate evolves somehow towards its stabilized value. This period corresponds to evolution of the contact angles and near-wall interface velocities from their static values (not moving interface) towards certain stabilized values corresponding to nonzero interface velocity.
The times needed for stabilization of the measured flowrate were investigated. The stabilization time was defined as the time needed for the measured flowrate to achieve a deviation from its converged value smaller than 0.1 %. This time depends on parameters of the chosen contact angle model. E.g. for

a real flowrate of 1 mL/h this time was determined to be around 89 s for Seeberg model of the contact angle. For other flowrates the stabilization time t_s can be determined as

$$t_s = \left(\frac{Q}{Q_i}\right)^{-0.58} t_{si}$$

where t_{si} is certain known value of stabilization time for certain value of flowrate Q_i (e.g. $t_{si} = 89s$ for $Q_i = 1mL/h$).

Next the pulsating flows were investigated. Sinusoidal and triangular oscillations were considered. The flows were described by three parameters – mean volumetric flowrate Q_0, period T and relative amplitude A_r which is defined as ratio of amplitude and mean volumetric flowrate. The considered ranges of these parameters were $Q_0 = 0.001 \ldots 10\ mL/h;\ T = 5s;\ A_r = 0.1 \ldots 0.9$.
The same parameters were investigated for the measured flowrate which is obtained by time derivative of the scale reading. The differences between the parameters of the real and the measured flowrate were examined.
The period of the oscillations T remains unaffected by the buoyancy of the capillary forces and therefore it is the same for the real and measured flowrate.
The mean volumetric flowrate Q_0 can differ for the real and measured case e.g. because of buoyancy force. This shift appears also in constant flow case since the buoyancy force grows with time during filling of the beaker and therefore contributes to the time derivative of the scale reading. The quantification of the shift in case of pulsating flow was not investigated in detail in this work but it is reasonable to assume that the magnitude of the effect is similar as in the stationary case.
The relative amplitude A_r was found to be larger for the measured flowrate then for the real one. The difference was between 7.0 % and 8.6 % for all range of parameters investigated. For periods other than $T = 5s$ the difference does not change much as it was proven analytically.

The results obtained within this work should be compared with experimental results obtained by DTI in order to verify correctness of the model and its conclusions. The results of the numerical analysis could be also fine-tuned based on experiments of DTI which can give better estimations of the parameters of the model. The assumptions of the MATLAB model could be also verified by a CFD simulation e.g. in OpenFoam which can give an information about influence of the fluid velocity distribution to the capillary and buoyancy forces.

References

[1] J. Geršl, *Uncertainty of flowrate for nano-flow standard of DTI – analytical and numerical evaluation*, EMRP project MeDD, D1.3.2 Final Report

[2] S. van Mourik, *Numerical modelling of the dynamic contact angle*, University of Groningen (2002), Master Thesis